

## Site-Specific DNA–Doxorubicin Conjugates Display Enhanced Cytotoxicity to Breast Cancer Cells

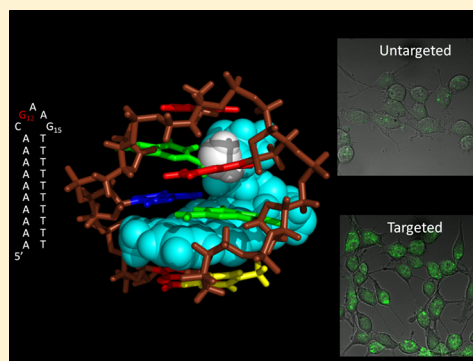
Christopher H. Stuart,<sup>†,‡</sup> David A. Horita,<sup>§,⊥</sup> Michael J. Thomas,<sup>§</sup> Freddie R. Salsbury, Jr.,<sup>||</sup> Mark O. Lively,<sup>§</sup> and William H. Gmeiner<sup>\*,†,‡</sup>

<sup>†</sup>Department of Cancer Biology, <sup>‡</sup>Department of Molecular Medicine and Translation Science, Wake Forest School of Medicine, and <sup>§</sup>Department of Biochemistry, Wake Forest School of Medicine, Winston-Salem, North Carolina 27157, United States

<sup>||</sup>Department of Physics, Wake Forest University, Winston-Salem, North Carolina 27109, United States

### S Supporting Information

**ABSTRACT:** Doxorubicin (Dox) is widely used for breast cancer treatment but causes serious side effects including cardiotoxicity that may adversely impact patient lifespan even if treatment is successful. Herein, we describe selective conjugation of Dox to a single site in a DNA hairpin resulting in a highly stable complex that enables Dox to be used more effectively. Selective conjugation of Dox to G15 in the hairpin loop was verified using site-specific labeling with [2-<sup>15</sup>N]-2'-deoxyguanosine in conjunction with [<sup>1</sup>H-<sup>15</sup>N] 2D NMR, while 1:1 stoichiometry for the conjugate was validated by ESI-QTOF mass spectrometry and UV spectroscopy. Molecular modeling indicated covalently bound Dox also intercalated into the stem of the hairpin and stability studies demonstrated the resulting Dox-conjugated hairpin (DCH) complex had a half-life >30 h, considerably longer than alternative covalent and noncovalent complexes. Secondary conjugation of DCH with folic acid (FA) resulted in increased internalization into breast cancer cells. The dual conjugate, DCH-FA, can be used for safer and more effective chemotherapy with Dox and this conjugation strategy can be expanded to include additional anticancer drugs.



### INTRODUCTION

Doxorubicin (Dox) is widely used for treating breast cancer and other malignancies; however, serious toxicities, including an occasionally lethal cardiotoxicity, counter the therapeutic benefit of Dox, resulting in a search for chemical modifications that attenuate systemic toxicities while maintaining strong antitumor activity.<sup>1</sup> The principal cytotoxic mechanism of Dox is poisoning of DNA topoisomerase 2 (Top2) which results in generation of lethal DNA double strand breaks (DSBs).<sup>2</sup> Dox also undergoes REDOX cycling and increases oxidative stress following cell uptake. Recent studies have indicated that Dox cardiotoxicity results from an on-target effect, the poisoning of Top 2 in cardiomyocytes.<sup>3</sup> Hence, strategies to improve the therapeutic index of Dox require prolonged sequestration of Dox while in circulation and efficient Dox release following selective uptake into targeted cancer cells. We describe here a new approach for Dox delivery to cancer cells that takes advantage of the selective chemical reactivity of a single-site in a DNA hairpin to create a novel Dox-conjugated DNA hairpin (DCH) with favorable Dox retention and release properties and that is targeted to breast cancer cells via folic acid conjugation.

DNA is central to biological function as the repository of genetic information, but DNA also has tremendous potential as a material with diverse potential functions, including drug delivery. Our laboratory has demonstrated the utility of DNA for delivery of cytotoxic nucleotide analogs with F10, a polymer

of the thymidylate synthase (TS) inhibitory nucleotide 5-fluoro-2'-deoxyuridine-5'-O-monophosphate (FdUMP) displaying enhanced antileukemic activity and reduced systemic toxicity relative to conventional fluoropyrimidine drugs such as 5-fluorouracil (5-FU).<sup>4,5</sup> We recently demonstrated the potential for DNA hairpins to be useful for drug delivery with involvement of both the major and minor grooves as well as the duplex region of the hairpin. We have shown that cytotoxicity can be modulated by inclusion of minor groove binding ligands, such as netropsin or distamycin, while Zn<sup>2+</sup>, a metal ion that displays anticancer activity, can occupy the major groove in DNA hairpins appropriately substituted with FdU nucleotides in the stem.<sup>6,7</sup> Hence, not only are the chemical properties of DNA of potential use for drug delivery, but its structural diversity may also be utilized for drug delivery applications.

Dox interacts with DNA via intercalation of the tetracene ring system between the planar base pairs of duplex DNA and occupation of the minor groove by the daunosamine sugar moiety.<sup>8</sup> Noncovalent binding of Dox to DNA is, however, readily reversible, and noncovalent complexes have relatively short half-lives ( $t_{1/2} \sim$  minutes). Nonetheless, in clinical trials noncovalent association of Dox with calf-thymus DNA reduced

Received: November 25, 2013

Revised: January 22, 2014

Published: January 22, 2014

Dox cardiotoxicity and improved the therapeutic index.<sup>9</sup> Dox also forms covalent adducts with DNA that are more stable but require an aldehyde precursor to link the daunosamine sugar of Dox to the exocyclic amine of guanine with the reaction proceeding via a Schiff base intermediate.<sup>10,11</sup> Dox–DNA covalent adducts are more cytotoxic than noncovalent complexes, and covalent adducts have been synthesized and used as end-points in studies of anthracycline cytotoxicity.<sup>12</sup> Formaldehyde is used in the formation of Dox–DNA adducts, and exogenous formaldehyde promotes Dox covalent adduct formation to genomic DNA. Dox–formaldehyde conjugates have been prepared and used for delivery of an activated form of Dox that favors covalent adduct formation to genomic DNA.<sup>13</sup>

We describe here the synthesis of a covalent conjugate of Dox to a single site of a DNA hairpin and demonstrate that this conjugate can be targeted to breast cancer cells. Dox covalent binding to DNA occurs primarily at N2 of guanines with sequence specificity for 5'-dGpC sites, suggesting a 3D conformation that facilitates covalent binding.<sup>14</sup> Our studies utilized a 25mer DNA hairpin that included a GAA hairpin-promoting sequence closed by a CG base pair with the stem consisting of 10 dA-dT base pairs (Figure 1). Although the hairpin included two dG sites, using 2D NMR in conjunction with site-specific labeling we determined only G15 in the GAA hairpin promoting motif formed a covalent adduct with Dox (Figure 2). Molecular modeling suggested that G15 N2 was not engaged in alternative interactions stabilizing the hairpin and that the tetracene ring system intercalated between the CG and first AT base pairs (Figure 3). The Dox-conjugated hairpin was exceedingly stable with a half-life of ~30 h at physiological pH while the noncovalent complex had a half-life of minutes (Figure 4). Dox was however efficiently released at the acidic pH of endosomes following cell uptake (Figure 5). Folic acid conjugation of the hairpin resulted in cell-specific uptake into breast cancer cells and selective cytotoxicity toward targeted cells (Figure 6). These results demonstrate the utility of DNA hairpin conjugates for the improved delivery of Dox and other anticancer drugs.

## ■ EXPERIMENTAL SECTION

**Materials.** All nonlabeled hairpin DNA sequences were synthesized by IDT (Coralville, Iowa, USA). Isotopically labeled hairpins were synthesized by the DNA core lab at Wake Forest University. Clinical samples of doxorubicin (Dox) used for cell assays and DCH synthesis were obtained from the Wake Forest Baptist hospital pharmacy. Cu<sup>2+</sup>-Tris[(1-benzyl-1H-1,2,3-triazol-4-yl)methyl]amine (Cu<sup>2+</sup>-TBTA) was obtained from Lumiprobe (Hallandale Beach, Florida, USA). All media for cell culture was obtained from the Wake Forest University Cell and Viral Vector Core Lab. All other chemicals were obtained from Sigma-Aldrich and used as received.

**Synthesis of DCH.** A 0.37% (by weight) solution of formaldehyde was prepared by dissolving paraformaldehyde in Dulbecco's Phosphate Buffered Saline without calcium or magnesium (PBS) pH 7.4. Doxorubicin was added to 4 °C formaldehyde–PBS to obtain a final doxorubicin concentration of 250 μM. DNA hairpin loops were prepared as previously reported<sup>6</sup> by heating and flash-cooling of the DNA to favor intramolecular hairpin formation over dimerization. Hairpins were added to the Dox–formaldehyde solution to obtain a final hairpin concentration of 100 μM. Reactions were allowed to proceed at 10 °C in the dark for 48 h. DCHs were purified by

extracting twice with phenol/chloroform and twice with chloroform. This extraction removes unreacted dox from the solution. After extraction, DCHs were ethanol-precipitated and recovered by centrifugation. Pellets were rinsed twice with 70% ethanol and 100% ethanol to remove any residual formaldehyde. Pellets were then evaporated to dryness under reduced pressure. The red–pink pellets were then resuspended in water. A Beckman Coulter DU 800 was used to measure absorption at 260 nm. Yields were typically 70–80% for the conjugate as measured by UV absorbance at 260 nm. All products were stored at –20 °C.

**Synthesis of Alkyne Functionalized Folic Acid.** Alkyne functionalized folic acid was synthesized similarly to previously reported methods.<sup>15,16</sup> Briefly, folic acid (100 mg, 0.227 mmol) was dissolved into 10 mL of DMF and stirred with a magnetic stirrer and cooled in an ice bath for 30 min before proceeding. 1-Ethyl-3-(3-dimethylaminopropyl)carbodiimide HCl (EDC) (38.7 mg, 0.249 mmol) was added to the stirred solution and allowed to react for 30 min. *N*-Hydroxysuccinimide (NHS) (31.4, 0.272 mmol) was then added to the reaction vessel and stirred for an additional 30 min. Propargyl amine (25 mg, 0.454 mmol) was then added to the reaction, which was warmed to room temperature and allowed to react for 24 h. 10 mL of 1:1 diethyl ether/chloroform was added to the reaction vessel, which precipitated the yellow–orange product. This was collected and washed three times with chloroform, diethyl ether, and water. The product was dried under vacuum overnight. Yield 69 mg (64%). <sup>1</sup>H NMR (DMSO-*d*<sub>6</sub>, ppm): 11.06 (–OH), 8.64 (Pteridine C<sub>7</sub> H), 8.29–8.24 (–CONH–CH<sub>2</sub>C≡CH), 8.04 (–CONHCHCO<sub>2</sub>H), 7.67–7.65 (Ph–C<sub>2</sub>H and Ph–C<sub>6</sub>H), 6.94 (–NH<sub>2</sub>), 6.64 (Ph–C<sub>3</sub>H and Ph–C<sub>5</sub>H), 4.48 (Pteridine C<sub>6</sub>–CH<sub>2</sub>NH–Ph), 4.31 (–CONHCHCO<sub>2</sub>H), 3.81 (–CONH–CH<sub>2</sub>C≡CH), 3.08 (–CONH–CH<sub>2</sub>C≡CH), 1.98–1.96 (–CHCH<sub>2</sub>CH<sub>2</sub>), 1.87–1.85 (–CHCH<sub>2</sub>CH<sub>2</sub>, 2H).

**Synthesis of FA-DCH.** Hairpin with a 5' terminal azide was used for the synthesis of FA-DCH. 45 μL of a 100 μM solution of the hairpin was added to a 500 μL centrifuge tube. To this 10 μL (pH = 7, 2 M) of triethylamine/acetic acid buffer was added and mixed. 45 μL DMSO was then added to the solution and mixed well. 4.5 μL of a 10 mM solution of alkyne functionalized folic acid was added to the solution, mixed, and bubbled with Ar for 15 min. 10 μL of 5 mM ascorbic acid in water was added to the solution followed by 5 μL of Cu<sup>2+</sup>-TBTA. The reaction was mixed and bubbled with Ar for 15 min before sealing the tube and being placed in the dark at room temperature for 24 h. FA-DCH was purified similarly to DCH. The hairpin was precipitated using 4× volume ethanol and 25 μL PBS and was cooled at –20 °C for 30 min. The hairpin was recovered by centrifugation at 13 000 × *g* for 30 min. The pellet was rinsed 2× with 70% EtOH and 2× with 100% EtOH and dried under reduced pressure. The pellet was resuspended with 500 μL PBS and was dialyzed against PBS using a Slide-a-Lyzer 2 kDa MW cutoff dialysis cassette (Pierce) for 6 h to remove unreacted propargyl-folate. The retained solution was collected and quantified via UV–vis spectroscopy, with a final yield of 53%.

**Doxorubicin–DNA Conjugate Ratio Measurements.** DNA samples were prepared to 10 μM in dH<sub>2</sub>O and absorbencies were measured from 200 to 800 nm using a Beckman Coulter DU800 spectrophotometer. A standard curve of Dox was established between 1 μM and 10 μM by using absorbance at 494 nm. To assess the amount of Dox covalently bound to DNA, the samples were heated to 85 °C before

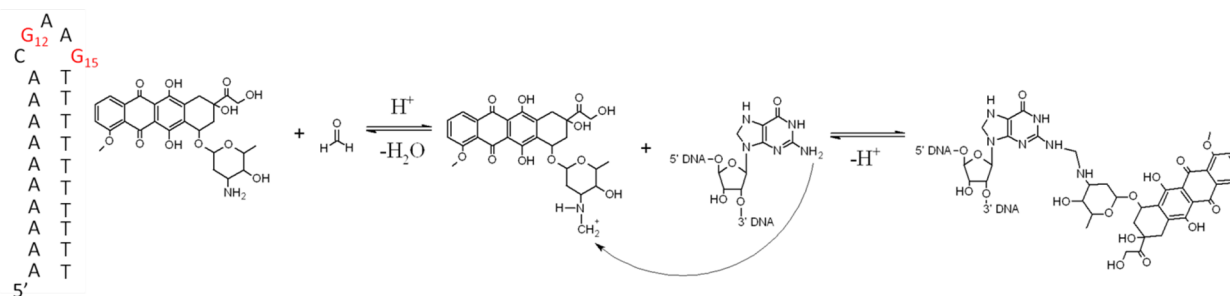


**Figure 1.** Reversible reaction between Doxorubicin and the exocyclic amino of Guanine in DNA mediated through formaldehyde. Red “G” in the secondary structure of the hairpin denotes potential sites of Dox reactivity.

measuring the absorbance at 494 nm. The 260 nm wavelength was used to determine the DNA content in the sample and to determine the Dox:DNA ratio.

**Mass Spectrometry.** Negative ion mass spectra were acquired using a Waters Q-TOF API-US mass spectrometer equipped with an Advion Nanomate source. Samples were diluted to about 5  $\mu\text{M}$  with methanol/water/2-propanol (49:49:2, v:v:v). Backing pressure and sprayer voltage were optimized for each analysis, but were usually about 0.8 psi and 1.2 kV, respectively. The cone voltage was 35 V. The scan range from 525  $m/z$  to 1600  $m/z$  with an acquisition time of 1.2 s. Spectra were summed for 0.5 min for MaxEnt transform. The nucleotide GCATCCTGGAAAGCTACCTT,  $M^- = 6366.1$ , at 0.6  $\mu\text{M}$  was used to monitor instrument performance. Spectra were analyzed using MassLynx 4.0.

**NMR Spectroscopy.** NMR samples were prepared in 50 mM sodium phosphate buffer, pH 7.0, with 10%  $\text{D}_2\text{O}$ , and a final volume of 250  $\mu\text{L}$ . All NMR spectra were acquired using a Bruker Avance 600 MHz spectrometer at 10  $^\circ\text{C}$  using a TXI Cryoprobe. NOESY spectra were acquired with a 100 ms mixing time and 3–9–19 Watergate water suppression with a 220  $\mu\text{s}$  interpulse delay. HSQC spectra were acquired using a 110  $\mu\text{s}$  3–9–19 interpulse delay and the  $^{15}\text{N}$  transmitter set to 150 ppm for imino groups and to 75 ppm for amino groups (indirectly referenced to water at 4.7 ppm). Data were processed using NMRPipe<sup>17</sup> and analyzed using NMRView.<sup>18</sup>

**3D Modeling of DCH.** A PDB file of the hairpin molecule was obtained from the Protein Data Base under entry 1JVE.<sup>19</sup> A PDB file of Dox was obtained from the Protein Data Base under entry DM2. Files were loaded into Pymol,<sup>20</sup> and the hairpin was modified to contain only 5'-ACGAAGT-3'. The models were then manipulated spatially to allow for a covalent bond to form between the N2 amino of G12 and the daunosamine of Dox. Hydrogens were added to the entire model using the Molefactory plugin vmd.<sup>21</sup> The doxorubicin was then geometry optimized in the presence of the DNA using PM6<sup>22</sup> as implemented in Gaussian 09.<sup>23</sup>

**Dox Transfer from DCH.** Samples of 2.5  $\mu\text{M}$  (approximately 2  $\mu\text{g}$  in 100  $\mu\text{L}$ ) DCH, doxorubicin, or hairpin +doxorubicin were prepared in DPBS with or without a 100-fold by weight (200  $\mu\text{g}$ ) excess of Salmon Sperm DNA and incubated at 37  $^\circ\text{C}$ . Fluorescence intensity was determined by Typhoon-9210 variable mode imager with excitation set to 532 nm and the emission filter at 610 nm.

**Acid Dissociation of Dox from DCH.** DCH was suspended in either pH 7.4 PBS or pH 4 PBS buffer and incubated at 37  $^\circ\text{C}$  for 1 h. After incubation, the solutions were extracted with 2 $\times$  volume phenol/chloroform and twice with 2 $\times$  volume chloroform. The absorbance of the aqueous phase

at 498 nm was measured. The experiment was repeated in triplicate. The results were normalized to the pH 7.4 sample with error bars representing the standard deviation of the mean of the three replicates.

**Microscopy.** 4T1 cells were seeded at 20 000 cells/well in 8-well Lab-Tek II chambered #1.5 German Coverglass System (Thermo Fisher Scientific, Waltham, MA), and incubated at 37  $^\circ\text{C}$  under 5%  $\text{CO}_2$  for 24 h prior to treatment. Cells were incubated with 1  $\mu\text{M}$  of DCH, FA-DCH, or Dox in DMEM medium with 10% dialyzed fetal bovine serum for either 1 or 4 h at 37  $^\circ\text{C}$ . Cells were then washed with fresh media and Dulbecco's PBS. Cells were visualized using a Zeiss LSM510 confocal microscope (Carl Zeiss, Oberkochen, Germany) using Dox as the fluorescent probe. Internalization of Dox was quantified using ImageJ software with at least 30 observations per treatment. Fluorescence intensity values were then converted to % controls using nontreated cells. The mean of the intensities was found and standard deviation was determined. Significance was determined using a two-tailed Student's  $t$  test.

**Cytotoxicity.** 4T1 cells were grown in DMEM media containing 10% dialyzed FBS and 1% penicillin/streptomycin, at 37  $^\circ\text{C}$  and 5%  $\text{CO}_2$ . 4T1 cells were plated at 5000 cell per well in 96 well plates in 100  $\mu\text{L}$  media and incubated for 24 h. Cells were treated with 200 nM of either DCH, Dox, or FA-DCH for 72 h with 4 replicates of each treatment used to determine means and standard deviation. CellTiter-Glo luminescent cell viability assay (Promega) was implemented according to the manufacturer's protocol. Significance was determined using a two-tailed Student's  $t$  test.

## RESULTS

**Site-Specific Dox Conjugation of a DNA Hairpin.** The DNA hairpin used for these studies includes two guanines (Figure 1) either of which may in principle be a site for Dox conjugation. Dox conjugates have been previously described for guanines engaged in GC base pairs; however, the chemical reactivity of the GAA sequence motif used to promote intramolecular hairpin formation has not been previously investigated. UV spectroscopy studies (Figure 2A) revealed that Dox conjugation occurred with 1:1 stoichiometry even in cases where reaction conditions permitted formation of conjugates of 2:1 or higher stoichiometry. The 1:1 stoichiometry of the conjugates was further demonstrated using ESI-QTOF mass spectrometry (Figure 2B). Mass spectrometry analysis also confirmed that the conjugation occurred via a methylene bridge derived from formaldehyde consistent with reaction proceeding via a Schiff base intermediate. To determine to what extent each of the two guanines in the hairpin were adducted in the



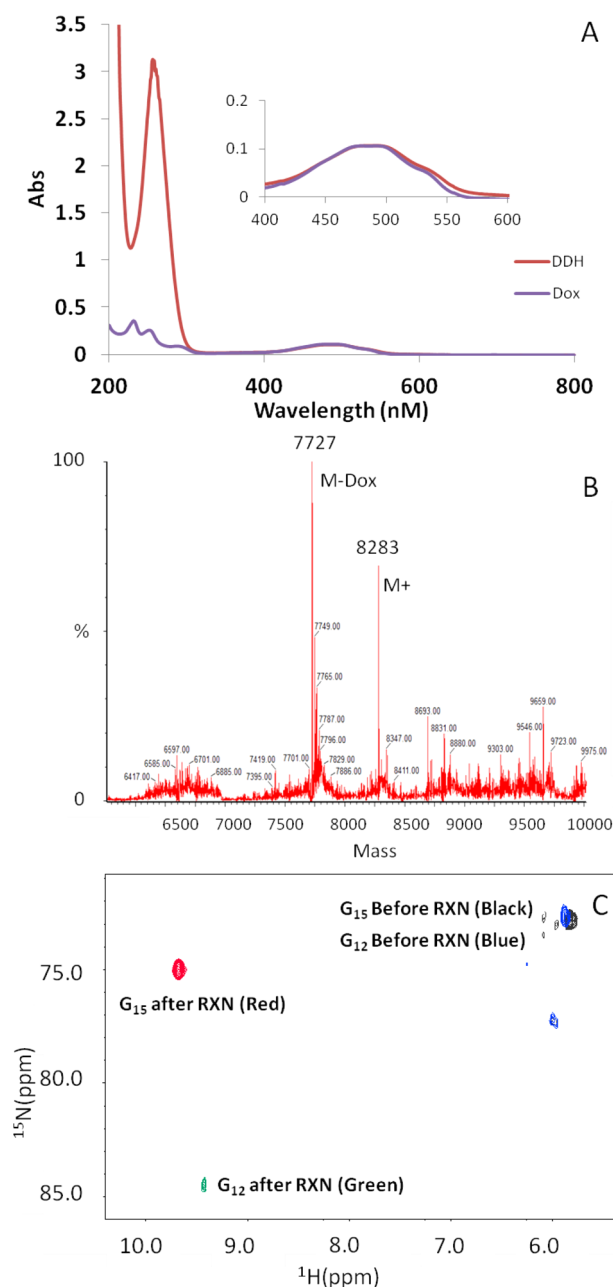


**Figure 2.** (A) UV-vis absorbance spectra for equimolar amounts of Dox and DCH. Equal absorbance at 480 nm is consistent with the DCH complex being of 1:1 stoichiometry. (B) M-Dox peak of MW 7727 corresponds to the unreacted parent DNA, while the M+ peak of MW 8283 is obtained by the addition of Dox (MW 543) and  $\text{CH}_2$  (MW 14)  $-2\text{H}$  lost as water. (C) Overlay of  $^1\text{H}$ - $^{15}\text{N}$  HSQC displaying the N2 of G12 and G15 from two independent singly labeled samples. Blue and green peaks represent the G12 amino before and after reaction with Dox, respectively. Black and red peaks represent the G15 amino before and after reaction, respectively.

conjugate, we synthesized the hairpin site-specifically  $^{15}\text{N}$ -labeled at either G12 or G15 and formed Dox conjugates with both species and analyzed each for chemical adduction based on chemical shift changes in 2D [ $^1\text{H}$ - $^{15}\text{N}$ ] NMR spectra (Figure 2C). Substantial  $^{15}\text{N}$  chemical shift changes were only detected for the hairpin labeled at G12 (72.6  $\rightarrow$  84.5 ppm), consistent with this site selectively undergoing chemical modification upon adduct formation. This represents the first

time that we are aware of that Dox covalent bonding has been observed in a hairpin loop region of DNA. G15, which is engaged in a GC base pair that closes the loop, underwent substantial change in  $^1\text{H}$  (5.8  $\rightarrow$  9.7 ppm) but not  $^{15}\text{N}$  chemical shift (72.8  $\rightarrow$  75.0 ppm) consistent with this site undergoing changes in chemical environment, but not chemical structure, upon Dox conjugation. Subsequent molecular modeling studies revealed the CG base pair was stacked with the tetracene ring system of Dox in the resulting conjugate (vide infra).

**Molecular Model of Dox-Conjugated Hairpin.** We then sought to create a working model for the structure of the Dox-

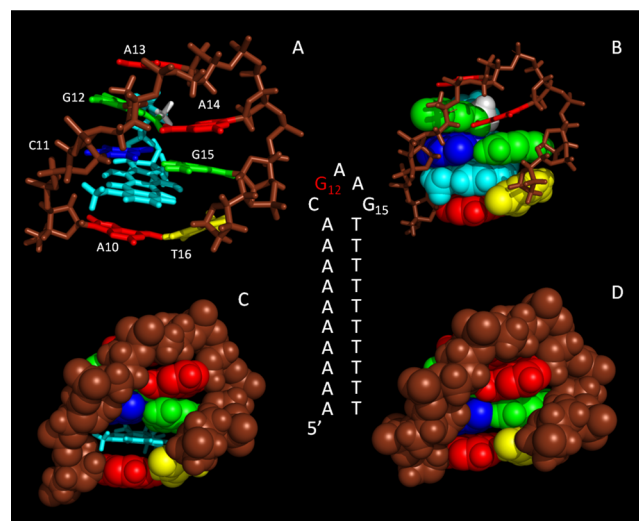


**Figure 3.** Secondary structure and molecular model of the DCH. Dox is bound to N2 of G12 and intercalated between the G15:C11 and A10:T16 base pairs. The lower 9 AT base pairs of the stem have been truncated for simplicity. Structures are colored as follows: guanine, green; adenine, red; thymine, yellow; cytosine, blue; Dox, light blue; methylene linker, white; DNA backbone, brown. (A–C) 3D modeling of the DCH structure. (D) 3D model of the unreacted hairpin.

conjugated hairpin (Figure 3) using the data collected from the  $^{15}\text{N}$ -edited 2D NMR and using a NMR structure of the hairpin loop characterized by Ulyanov et al.<sup>19</sup> as the starting point for model development. The hydrogen shifts of G15 could be caused by intercalation of Dox in the covalent complex, as shifts of amino protons to  $\sim 10$  ppm have been attributed to increased hydrogen bonding in quadruplex DNA.<sup>24</sup> Preliminary data also showed that the amino of G15 displayed several NOEs consistent with Dox localizing in the stem region of the hairpin (SI 1). Pymol was used to edit the DNA from the previous NMR structure to contain only the loop region and the first AT base pair. We then manipulated a model of Dox into a position that brought the amino hydrogens of G12 and Dox into close proximity, allowing for the formation of a methylene bridge between the amino nitrogens. This placement also allowed Dox to intercalate between the C11-G15 base pair and the first AT base pair in the stem of the DNA (Figure 3A,B). Modeling revealed that the simultaneous covalent binding at G12 and intercalation of Dox between the A10:T16 and C11:G15 occurred with minimal distortion to the structure of the hairpin loop (Figure 3C,D). The daunosamine sugar is of appropriate dimensions to span the distance between the sites of covalent binding and intercalation and the amino group of G12 is not engaged in hydrogen

bonding interactions that contribute significantly to the structure and stability of the hairpin loop. Intercalation of the tetracene ring alters local base stacking for the proximal base pairs but does not disrupt hydrogen bonding interactions (Figure 3D).

**Stability of Dox–Hairpin Conjugate.** We hypothesized that covalent binding of Dox would allow for the Dox-conjugated hairpin to serve as a delivery vehicle with improved pharmacological properties and reduced systemic toxicities relative to conventional Dox. In order for the hairpin to act as an efficient delivery vehicle, Dox must remain stably bound under physiological conditions, but also undergo intracellular release and transfer to genomic DNA. Interestingly, Dox retains most of its fluorescent activity in the hairpin, but not in larger DNA molecules which are known to quench the fluorescence of the drug<sup>26</sup> (SI 2). We hypothesized that as the Dox–hairpin bond is hydrolyzed, the free Dox could intercalate into larger DNA molecules, quenching the fluorescence. Using the difference in fluorescence between hairpin bound Dox and Dox intercalated into DNA, we can measure the half-life of the Dox–hairpin bond. We developed an assay to quantify the transfer of Dox from the hairpin to genomic DNA under physiologic conditions. This assay is based on the difference in fluorescence of Dox in the context of the hairpin conjugate relative to genomic DNA. The hairpin conjugate, free-Dox, or the noncovalent complex (e.g., hairpin+Dox) were mixed with 100-fold excess of salmon sperm DNA (spDNA; w/w) to simulate genomic DNA. Reactions were incubated at 37 °C with fluorescence quenching measured over 48 h. No fluorescence loss was observed in samples that lacked spDNA, while fluorescence was fully quenched within one hour following addition of spDNA for both free Dox and the noncovalent complex. The rate of loss of fluorescence quenching was, however, significantly reduced for the hairpin conjugate with 50% quenching occurring at 30.4 h (Figure 4).

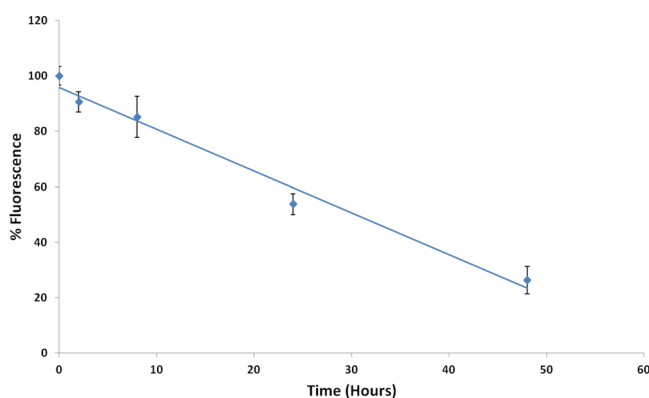


**Figure 4.** Fluorescence quenching of DCH displays a ~50% reduction in fluorescence after 30 h, while noncovalent complexes display greater than 50% reduction in fluorescence within 1 h (data not shown). Error bars represent standard deviation of the mean of three measurements. Assuming zero-order kinetics, the rate constant is  $k = 1.15 \times 10^{-11}$  M/s.

Using  $t_{1/2}$  of 30.4 h and assuming zero-order kinetics, the rate constant is  $1.15 \times 10^{-11}$  M/s. Given that the noncovalent hairpin +Dox complex undergoes rapid quenching, intercalation into the hairpin cannot be solely responsible for the increased chemical stability of the hairpin conjugate. Covalent Dox dimers formed using formaldehyde have been shown to be

readily hydrolyzable under physiological conditions, resulting in complete disassociation of Dox and formaldehyde release within ~15 min.<sup>13</sup> Thus, it is likely that a combination of both intercalation and covalent bonding is responsible for the substantially increased stability for the Dox-conjugated hairpin relative to the noncovalent complex and alternative Dox covalent complexes. We hypothesize that the covalent linkage acts as a tether between the Dox and DNA, and that when the bond is hydrolyzed, intercalation holds the resulting amine and Schiff-base in close proximity allowing for them to reform the covalent linkage. At physiological pH, equilibrium favors reforming the covalent complex, while at acidic pH, for example, in endosomes, equilibrium disfavors reforming the covalent linkage and instead results in release of Dox from the intercalated complex.

**Targeted Uptake and Enhanced Cytotoxicity to Breast Cancer Cells.** Cellular uptake of exogenous DNA can be highly efficient if uptake occurs via receptor-mediated processes. Our initial studies with the Dox-conjugated hairpin indicated uptake into breast cancer cells was less efficient than for F10, a single-stranded DNA investigated in our previous studies. As our previous studies demonstrated that conjugation with folic acid improved F10 uptake into drug-resistant colon cancer cells,<sup>25</sup> we investigated whether conjugating the Dox-hairpin at the 5'-terminus with folic acid would improve uptake into 4T1 breast cancer cells. Folic acid conjugation of the hairpin resulted in significantly increased cellular uptake relative to the nonconjugated hairpin based upon increased Dox fluorescence into 4T1 breast cancer cells (Figure 5). Dox fluorescence was initially localized in endosomes (SI 3) consistent with cellular internalization via an endocytic process and with release of Dox at the acidic pH of endosomes. Folic acid conjugation also increased the cytotoxicity of the Dox-conjugated hairpin toward 4T1 cells consistent with both improved cell uptake and efficient Dox release (Figure 6). The results demonstrate that, while the Dox-conjugated hairpin has markedly improved stability at physiological pH relative to the corresponding noncovalent complex, the conjugate is highly effective at the intracellular release of Dox following cell uptake.

## DISCUSSION

DNA is central to biology as the predominant carrier of genetic information; however, the physical and chemical properties of DNA make it highly useful as a material for numerous applications including use for drug delivery. These studies have demonstrated that a simple DNA hairpin that includes a “GAA” hairpin-promoting sequence provides a unique site for conjugation with the Top2-poisoning anticancer drug Dox. Conjugation occurs without disrupting stabilizing hydrogen bonding or base stacking interactions in the hairpin loop and allows for facile intercalation of the tetracene ring system of Dox between the first and second base pairs of the hairpin stem. The concurrent covalent linkage and intercalation of Dox in the hairpin results in formation of a complex that is highly stable at physiological pH. As noncovalent Dox–DNA complexes, presumably of greatly reduced chemical stability relative to the Dox-conjugated DNA hairpin described here have shown decreased toxicity relative to free Dox in human clinical trials,<sup>9</sup> hairpin conjugates may represent an improved approach for limiting Dox toxicity while preserving Dox efficacy.

A number of approaches have been described for improved Dox delivery while limiting systemic toxicities. The liposomal formulation Doxil, for example, has demonstrated clinical

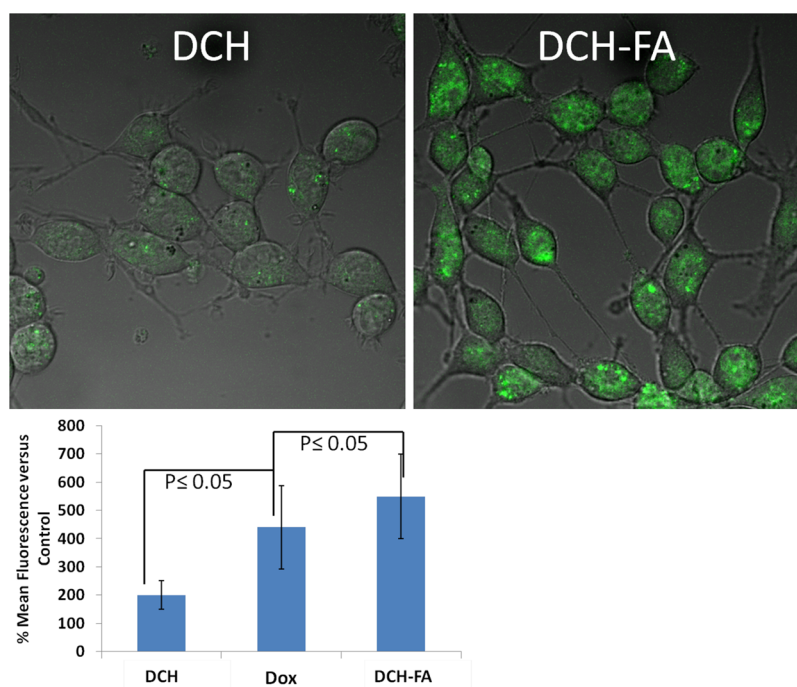


**Figure 5.** (A) Fluorescence microscopy of 4T1 cells treated with either untargeted or folate-targeted DCH. (B) Quantification of Dox fluorescence from 4T1 cells. Error bars represent standard deviation from the mean of at least 30 measurements. A Student's two-tailed *t* test was used to determine significance.

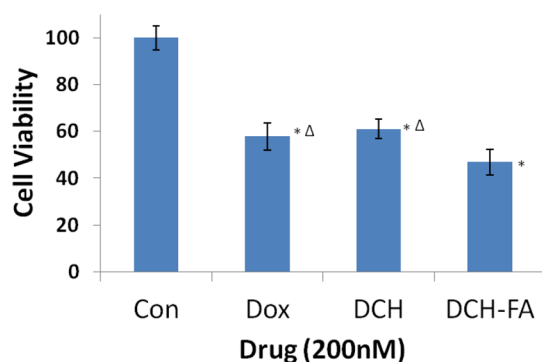


**Figure 6.** Targeting DCH with folic acid (DCH-FA) significantly increases the cytotoxicity of the DCH construct toward 4T1 breast cancer cells. Error bars represent standard deviation from the mean with four replicates of each condition. A Student's two-tailed *t* test was used to determine significance (i.e.,  $p < 0.05$ )—\*significantly different from control; Δsignificantly different from DCH-FA.

utility.<sup>27</sup> A variety of other nanoparticle-mediated drug delivery approaches have also been explored for improved Dox delivery.<sup>28–30</sup> DNA offers many advantages relative to alternative strategies. DNA is readily biodegradable and can be used for in vivo applications without activating an immune response. Further, the use of DNA for drug delivery allows for natural combination of diverse anticancer drugs of different classes. For example, our laboratory has pioneered the inclusion of cytotoxic nucleotide analogs into ssDNA<sup>4,5</sup> and more recently into DNA hairpins.<sup>6,7</sup> We have also shown that duplex or hairpin DNA can be used for delivery of minor groove binding ligands.<sup>6,7</sup> The present studies have extended this work to include covalent modification of DNA hairpins with simultaneous intercalation by DNA-targeting drugs, such as the Top2 poison Dox. Our studies have also shown that the major groove of DNA can be used for improved drug delivery

as our studies have shown that Zn<sup>2+</sup> complexation occurs in the major groove of FdU-substituted DNA hairpins.

Drug delivery is a multifaceted process that involves not only improved stability in circulation, but also specific uptake into targeted cells and ultimately release of drug following cell uptake. Our studies show that, as with previous studies with the single-stranded DNA F10, conjugation with folic acid improves uptake into targeted cancer cells.<sup>25</sup> Many cancer cells overexpress folate receptor as a consequence of increased nutrient requirements to support an elevated growth rate for the malignant phenotype.<sup>31</sup> These studies show cell uptake of a 25 nucleotide DNA hairpin can be significantly enhanced into 4T1 breast cancer cells through folic acid conjugation. Importantly, while the Dox-conjugated hairpin is highly stable at physiological pH, Dox release is favored at the acidic pH of endosomes following cell uptake. Dox is efficiently released from the hairpin following cell uptake and Dox retains potency as an anticancer drug. The results demonstrate that the DNA-conjugation strategy developed has the requisite components to be useful for Dox delivery in a clinical setting.

To our knowledge, this is the first report of the use of a Dox–DNA covalent conjugate to transfer Dox to DNA for potential therapeutic applications. The approach adopted has potential for greatly expanded drug delivery applications. For example, we have previously shown that FdU nucleotides can be embedded within this hairpin sequence and that the resulting hairpin is cytotoxic to prostate cancer cells.<sup>6,7</sup> As DNA polymers containing FdU nucleotides are Top1 poisons, the present system allows for creating complexes that deliver both FdU and Dox and that will simultaneously target Top1 and Top2. Simultaneous targeting of Top1 and Top2 has shown promise for clinical management of cancer, although this combination displays systemic toxicities.<sup>32,33</sup> Our studies show that folic acid conjugation can be used to improve uptake for DNA hairpin conjugates into breast cancer cells, and this is



expected to concomitantly reduce systemic toxicities. Studies are underway to evaluate these promising concepts in drug delivery. Future studies will focus on demonstrating advantages in cellular and animal models of cancer.

## CONCLUSIONS

The “GAA” sequence motif that promotes intramolecular DNA hairpin formation can be selectively conjugated to the Top2-poisoning anticancer drug Dox. The resulting conjugate is highly stable at physiological pH as a consequence of both covalent modification and intercalation of the tetracene ring system of Dox into the hairpin stem. Folic acid conjugation of the Dox-conjugated hairpin enhances uptake by 4T1 breast cancer cells. Dox is efficiently released at the acidic pH of endosomes following cell uptake demonstrating that the Dox-conjugated hairpin has both appropriate extracellular stability and intracellular lability well-suited for drug delivery applications. The DNA hairpin structural motif permits further development by inclusion of additional or alternative cytotoxic drugs, such as FdU or other cytotoxic nucleotide analogs demonstrating the multifunctional properties of DNA as a material for drug delivery science.

## ASSOCIATED CONTENT

### Supporting Information

NOESY NMR spectra of DCH, absorbance of DCH after acid extractions, and fluorescence microscopy of Dox endosomal uptake by 4T1 cells. This material is available free of charge via the Internet at <http://pubs.acs.org/>.

## AUTHOR INFORMATION

### Corresponding Author

\*Phone: (336) 716-6216. Fax: (336) 716-0255. E-mail: [bgmeiner@wakehealth.edu](mailto:bgmeiner@wakehealth.edu).

### Present Address

<sup>†</sup>David A. Horita, University of North Carolina Nutrition Research Institute, Kannapolis, NC 28081.

### Notes

The authors declare no competing financial interest.

## ACKNOWLEDGMENTS

The authors would like to thank Michael Samuel from the Wake Forest University Mass Spectrometry Core Lab for his help in obtaining all of the mass spectrometry data used in this research. Oligonucleotide syntheses were performed in the DNA Synthesis Core Laboratory at Wake Forest University School of Medicine. The DNA Synthesis and the Mass Spectrometry Cores are part of the Bioanalytical Core Laboratory supported in part by the Comprehensive Cancer Center of Wake Forest University. Funding was provided by Department of Defense Prostate Cancer Research Program (093606 to W.H.G.) and the Comprehensive Cancer Center of Wake Forest University Cancer Center Support Grant P30 CA012197 supporting the Bioanalytical Core Laboratory. The Waters Q-TOF mass spectrometer was purchased with funds from NIH Shared Instrumentation Grant 1S10RR17846. MS analyses were performed in the Mass Spectrometer Facility of the Comprehensive Cancer Center of Wake Forest University School of Medicine supported in part by NCI center grant SP30CA12197.

## REFERENCES

- (1) Elliott, P. (2006) Pathogenesis of cardiotoxicity induced by anthracyclines. *Semin. Oncol.* 33 (3Suppl8), S2–7.
- (2) Sordet, O., Khan, Q. A., Kohn, K. W., and Pommier, Y. (2003) Apoptosis Induced by Topoisomerase Inhibitors. *Curr. Med. Chem. Anti-Cancer Agents* 3, 271–290.
- (3) Zhang, S., Liu, X., Bawa-Khalife, T., Lu, L.-S., Lyu, Y. L., Liu, L. F., and Yeh, E. T. H. (2012) Identification of the molecular basis of doxorubicin-induced cardiotoxicity. *Nat. Med.* 18, 1639–1642.
- (4) Liao, Z.-Y., Sordet, O., Zhang, H.-L., Kohlhagen, G., Antony, S., Gmeiner, W. H., and Pommier, Y. (2005) A novel polypyrimidine antitumor agent FdUMP[10] induces thymineless death with topoisomerase I-DNA complexes. *Cancer Res.* 65, 4844–4851.
- (5) Pardee, T. S., Gomes, E., Jennings-Gee, J., Caudell, D., and Gmeiner, W. H. (2012) Unique dual targeting of thymidylate synthase and topoisomerase I by FdUMP[10] results in high efficacy against AML and low toxicity. *Blood* 119, 3561–3570.
- (6) Ghosh, S., Salsbury, F. R., Jr., Horita, D. A., and Gmeiner, W. H. (2011) Zn<sup>2+</sup> selectively stabilizes FdU-substituted DNA through a unique major groove binding motif. *Nucleic Acids Res.* 39, 4490–4498.
- (7) Ghosh, S., Salsbury, F. R., Jr., Horita, D. A., and Gmeiner, W. H. (2013) Cooperative stabilization of Zn(2+):DNA complexes through netropsin binding in the minor groove of FdU-substituted DNA. *J. Biomol. Struct. Dyn.* 31, 1301–1310.
- (8) Wang, A. H., Gao, Y. G., Liaw, Y. C., and Li, Y. K. (1991) Formaldehyde cross-links daunorubicin and DNA efficiently: HPLC and X-ray diffraction studies. *Biochemistry* 30, 3812–3815.
- (9) Trouet, A., and Jolles, G. (1984) Targeting of daunorubicin by association With DNA or proteins: a review. *Semin. Oncol.* 11 (4Suppl3), 64–72.
- (10) Zeman, S. M., Phillips, D. R., and Crothers, D. M. (1998) Characterization of covalent Adriamycin-DNA adducts. *Proc. Natl. Acad. Sci. U.S.A.* 95, 11561–11565.
- (11) Cutts, S. M., Parker, B. S., Swift, L. P., Kimura, K. I., and Phillips, D. R. (2000) Structural requirements for the formation of anthracycline-DNA adducts. *Anti-Cancer Drug Des.* 15, 373–386.
- (12) Swift, L. P., Cutts, S. M., Rephaeli, A., Nudelmann, A., and Phillips, D. R. (2003) Activation of adriamycin by the pH-dependent formaldehyde-releasing prodrug hexamethylenetetramine. *Mol. Cancer Ther.* 2, 189–198.
- (13) Post, G. C., Barthel, B. L., Burkhart, D. J., Hagadorn, J. R., and Koch, T. H. (2005) Doxazolidine, a proposed active metabolite of doxorubicin that cross-links DNA. *J. Med. Chem.* 48, 7648–7657.
- (14) Phillips, D. R., White, R. J., and Cullinane, C. (1989) DNA sequence-specific adducts of adriamycin and mitomycin C. *FEBS Lett.* 246, 233–240.
- (15) Lee, R. J., and Low, P. S. (1994) Delivery of liposomes into cultured KB cells via folate receptor-mediated endocytosis. *J. Biol. Chem.* 269, 3198–3204.
- (16) Zhang, H., Cai, Z., Sun, Y., Yu, F., Chen, Y., and Sun, B. (2012) Folate-conjugated  $\beta$ -cyclodextrin from click chemistry strategy and for tumor-targeted drug delivery. *J. Biomed. Mater. Res. A* 100, 2441–2449.
- (17) Piotta, M., Saudek, V., and Sklenár, V. (1992) Gradient-tailored excitation for single-quantum NMR spectroscopy of aqueous solutions. *J. Biomol. NMR* 2, 661–665.
- (18) Delaglio, F., Grzesiek, S., Vuister, G. W., Zhu, G., Pfeifer, J., and Bax, A. (1995) NMRPipe: a multidimensional spectral processing system based on UNIX pipes. *J. Biomol. NMR* 6, 277–293.
- (19) Ulyanov, N. B., Bauer, W. R., and James, T. L. (2002) High-resolution NMR structure of an AT-rich DNA sequence. *J. Biomol. NMR* 22, 265–280.
- (20) *The PyMOL Molecular Graphics System*, v 1.5.0.4; Schrödinger, LLC.
- (21) Humphrey, W., Dalke, A., and Schulten, K. (1996) VMD: visual molecular dynamics. *J. Mol. Graphics* 14, 33–38.
- (22) Stewart, J. J. P. (2007) Optimization of parameters for semiempirical methods V: Modification of NDDO approximations and application to 70 elements. *J. Mol. Model.* 13, 1173–1213.

(23) Frisch, M. J., Trucks, G. W., Schlegel, H. B., Scuseria, G. E., Robb, M. A., Cheeseman, J. R., Scalmani, G., Barone, V., Mennucci, B., Petersson, G. A., Nakatsuji, H., Caricato, M., Li, X., Hratchian, H. P., Izmaylov, A. F., Bloino, J., Zheng, G., Sonnenberg, J. L., Hada, M., Ehara, M., Toyota, K., Fukuda, R., Hasegawa, J., Ishida, M., Nakajima, T., Honda, Y., Kitao, O., Nakai, H., Vreven, T., Montgomery, Jr., J. A., Peralta, J. E., Ogliaro, F., Bearpark, M., Heyd, J. J., Brothers, E., Kudin, K. N., Staroverov, V. N., Kobayashi, R., Normand, J., Raghavachari, K., Rendell, A., Burant, J. C., Iyengar, S. S., Tomasi, J., Cossi, M., Rega, N., Millam, J. M., Klene, M., Knox, J. E., Cross, J. B., Bakken, V., Adamo, C., Jaramillo, J., Gomperts, R., Stratmann, R. E., Yazyev, O., Austin, A. J., Cammi, R., Pomelli, C., Ochterski, J. W., Martin, R. L., Morokuma, K., Zakrzewski, V. G., Voth, G. A., Salvador, P., Dannenberg, J. J., Dapprich, S., Daniels, A. D., Farkas, Ö., Foresman, J. B., Ortiz, J. V., Cioslowski, J., and Fox, D. J. (2009) *Gaussian 09*, rev A.1, Gaussian, Inc., Wallingford, CT.

(24) Bouaziz, S., Kettani, A., and Patel, D. J. (1998) A K cation-induced conformational switch within a loop spanning segment of a DNA quadruplex containing G-G-G-C repeats. *J. Mol. Biol.* 282, 637–652.

(25) Liu, J., Kolar, C., Lawson, T. A., and Gmeiner, W. H. (2001) Targeted drug delivery to chemoresistant cells: folic acid derivatization of FdUMP[10] enhances cytotoxicity toward 5-FU-resistant human colorectal tumor cells. *J. Org. Chem.* 66, 5655–5663.

(26) Bagalkot, V., Lee, I.-H., Yu, M. K., Lee, E., Park, S., Lee, J.-H., and Jon, S. (2009) A combined chemoimmunotherapy approach using a plasmid-doxorubicin complex. *Mol. Pharmaceutics* 6, 1019–1028.

(27) O'Brien, M. E. R., Wigler, N., Inbar, M., Rosso, R., Grischke, E., Santoro, A., Catane, R., Kieback, D. G., Tomczak, P., Ackland, S. P., Orlandi, F., Mellars, L., Alland, L., Tendler, C., et al. (2004) Reduced cardiotoxicity and comparable efficacy in a phase III trial of pegylated liposomal doxorubicin HCl (CAELYX/Doxil) versus conventional doxorubicin for first-line treatment of metastatic breast cancer. *Ann. Oncol.* 15, 440–449.

(28) Boyacioglu, O., Stuart, C. H., Kulik, G., and Gmeiner, W. H. (2013) Dimeric DNA aptamer complexes for high-capacity-targeted drug delivery using pH-sensitive covalent linkages. *Mol. Ther. Nucleic Acids* 2, e107.

(29) Janes, K. A., Fresneau, M. P., Marazuela, A., Fabra, A., and Alonso, M. J. (2001) Chitosan nanoparticles as delivery systems for doxorubicin. *J. Controlled Release* 73, 255–267.

(30) Chang, Y., Liu, N., Chen, L., Meng, X., Liu, Y., Li, Y., and Wang, J. (2012) Synthesis and characterization of DOX-conjugated dendrimer-modified magnetic iron oxide conjugates for magnetic resonance imaging, targeting, and drug delivery. *J. Mater. Chem.* 22, 9594.

(31) Russell-Jones, G., McTavish, K., McEwan, J., Rice, J., and Nowotnik, D. (2004) Vitamin-mediated targeting as a potential mechanism to increase drug uptake by tumours. *J. Inorg. Biochem.* 98, 1625–1633.

(32) Eder, J. P., Chan, V., Wong, J., Wong, Y. W., Ara, G., Northey, D., Rizvi, N., and Teicher, B. A. (1998) Sequence effect of irinotecan (CPT-11) and topoisomerase II inhibitors in vivo. *Cancer Chemother. Pharmacol.* 42, 327–335.

(33) Morgensztern, D., Baggstrom, M. Q., Pillot, G., Tan, B., Fracasso, P., Suresh, R., Wildi, J., and Govindan, R. (2009) A phase I study of pegylated liposomal doxorubicin and irinotecan in patients with solid tumors. *Chemotherapy* 55, 441–445.